Chirality

Determination of the Absolute Chirality of Adsorbed Molecules**

Roman Fasel, Joachim Wider, Christoph Quitmann, Karl-Heinz Ernst,* and Thomas Greber*

Pasteur's separation of the optical antipodes of ammonium sodium tartrate tetrahydrate in 1848 and the concept of the asymmetrically substituted carbon atom, introduced by van't Hoff and le Bel, marked the birth of stereochemistry.[1] Although the Fischer–Rosanoff convention based on D-(+)-glyceraldehyde got general acceptance,[2] it was not possible to link the optical rotary power to the absolute configuration of chiral molecules. In 1951, however, Bijvoet and co-workers determined the absolute configuration of (+)-sodium rubidium tartrate through anomalous X-ray scattering and showed that the arbitrary D-/L-convention matches reality.[3] Increasing computational power and improved quantum mechanical codes nowadays allow to connect chiroptical spectra with absolute configuration,[4] but this approach is still limited to relatively small or rigid molecules. Other methods for determining the absolute configuration, such as wetting or enantioselective adsorption on polar crystals[5] and measurements of the electric polarization in ferroelectric liquid crystals,[6] have been reported.

The conformation of chiral molecules adsorbed on a surface plays an important role in biomineralization[7] and in stereoselective heterogeneous catalysis.[8] For example, tartaric acid serves as chiral modifier for the enantioselective hydrogenation of β-ketoesters over supported nickel catalysts.[9] To gain deeper insight into the mechanisms of enantioselective surface chemistry and biomineralization, a detailed analysis of the local adsorbate structure is necessary.[10]

The absolute chirality of molecules adsorbed on surfaces has been inferred from scanning tunneling microscopy (STM) images.[11] However, in most cases of molecular adsorption it is very difficult to correlate the observed electron densities with the absolute atomic positions, and modeling of STM images requires extensive theoretical and computational effort.[12]

Herein we demonstrate that the absolute configuration of chiral molecules adsorbed on single-crystal surfaces can be determined in a straightforward fashion by means of angle-scanned X-ray photoelectron diffraction (XPD),[13] a method delivering direct real-space structural information. For our study we chose the classic tartaric acid molecule adsorbed on the Cu(110) surface. This adsorbate system has been studied in great detail.[14] At low coverages and after activation at 405 K, tartaric acid becomes doubly deprotonated, with the resulting bitartrate species[15a] forming long-range ordered chiral structures on the surface.[15b] Based on IR spectroscopy results, a local C_2 symmetry for the bitartrate adsorbate complex has been proposed.[14]

Figure 1 illustrates the basic principles of the XPD experiment for the case of the adsorbed bitartrate species.

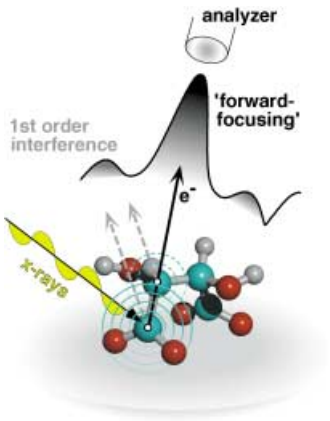

Figure 1. Illustration of the general principle of the angle-scanned XPD experiment. Angle-resolved photoelectron intensities from a particular emission line (e.g. C 1s) are collected over the complete hemisphere above the sample surface. At sufficiently high electron kinetic energies, the scattering of the outgoing electron wave (emanating from the C atoms in the present case) from the neighboring ion cores is strongly anisotropic. Most of the photoelectron intensity is scattered into the forward direction, giving rise to the so-called forward-focusing maxima in the angular distribution. Since these maxima occur in directions of nearby atoms, they allow a direct determination of the molecular structure.

When a molecule is illuminated by X-rays, photoelectrons are emitted from the atoms within the molecule and scattered by the surrounding atomic cores. At electron energies above about 500 eV, the scattering amplitude is mostly directed in the forward direction, which results in a strongly enhanced electron flux along the emitter–scatterer axis. This so-called forward-focusing effect allows a simple geometrical interpretation of the diffraction pattern where prominent intensity maxima can be identified with near-neighbor directions. The angular distribution of the photoelectrons therefore is, to a first approximation, a projected image of the atomic structure

[*] Dr. R. Fasel, Dr. K.-H. Ernst[+]
Swiss Federal Laboratories for Materials Testing and Research (EMPA)
Überlandstrasse 129, 8600 Dübendorf (Switzerland)
Fax: (+41) 1-823-4034
E-mail: roman.fasel@empa.ch
karl-heinz.ernst@empa.ch
Dr. J. Wider, Dr. T. Greber
Physik-Institut, Universität Zürich
Zürich (Switzerland)
Dr. J. Wider, Dr. C. Quitmann
Swiss Light Source, Paul-Scherrer Institute
Villingen (Switzerland)
[+] Current address: University of Washington
Department of Bioengineering
Seattle, WA 98195 (USA)

[**] This work was supported by grants from the Schweizerischer Nationalfonds and the Board of the Federal Institute of Technology (ETH Rat). The experiments were performed at the Swiss Light Source, Paul Scherrer Institute, Villigen (Switzerland).

 DOI: 10.1002/anie.200353311

around the photoemitters. Electrons from a particular emission line have their origin at the atoms selected by the choice of the emission line in the spectrum. This chemical sensitivity allows the corresponding XPD pattern to be associated with the local geometrical environment of the particular atom type chosen, for example, the local structure around the C atoms. Note that the source of the diffracted electron wave carrying structural information is within the molecule itself, and XPD therefore does not require long-range ordered structures, but is very sensitive to local order. This, together with its chemical selectivity, makes XPD to a powerful technique for surface structural investigations, which has been successfully applied to a variety of adsorbate systems.[16] However, only a few larger molecules, such as heptahelicene ($C_{30}H_{18}$)[17] and the fullerenes C_{60} and C_{70}[18] have been investigated. In particular, the low core-level photoelectron yield for submonolayers of the low atomic number atoms C, O, and N and their weak electron scattering power make XPD experiments on such molecular systems challenging. For the submonolayer coverage bitartrate/Cu(110) system herein, a conventional standard laboratory X-ray source did not yield C1s XPD patterns with sufficient signal-to-noise ratio even at prolonged counting times. To overcome this limitation, an endstation for full-hemispherical XPD experiments has been set up at a third-generation synchrotron radiation source[19] providing a high flux of monochromatic and polarized photons at energies well suited for XPD in the forward-focusing regime.

Figure 2 shows the experimental C 1s XPD patterns from the (*R*,*R*)- and (*S*,*S*)-bitartrate enantiomers adsorbed on the Cu(110) surface. The patterns are in a stereographic projection, where the center of the plot corresponds to normal emission of electrons (perpendicular to the surface) and the outer circle marks emission along the surface plane. The anisotropy of the patterns, that is, the difference between maximum and minimum intensity divided by maximum intensity, is of the order of 30%. The orientation of the Cu(110) substrate surface as determined from a substrate core-level XPD pattern (not shown) is indicated. Ten prominent intensity maxima are observed in the XPD patterns, and it is clear that the patterns from the two enantiomers are mirror images of each other. Furthermore, the chirality of each tartaric acid enantiomer is directly reflected in the corresponding XPD patterns which exhibit twofold rotational symmetry, but no mirror symmetry. As the strong intensity maxima correspond to emitter–scatterer directions and the emitters are known to be the carbon atoms, the conformation of the carbon backbone and the positions of the OH groups relative to the carbon skeleton are easily determined from the XPD patterns by applying purely geometrical arguments (Figure 2c and d).[20] By triangulation of the interatomic directions derived from the emission angles of the prominent forward-focusing peaks 1–5, molecular conformations are determined directly for the *R*,*R* and the *S*,*S* enantiomers (Figure 2c,d). Peak 1 is due to electrons emitted from a carboxylate carbon atom and forward focused along the C–C bond. Peak 2 corresponds to emission from the same carbon atom but scattering by the β carbon atom. Most important, peaks 3, 4 and 5 are fingerprints of the absolute configuration of the respective molecule: they are due to scattering from the hydroxy oxygen atoms, and locate the position of these oxygen atoms with respect to the carbon skeleton, hence they directly reflect the absolute configuration.

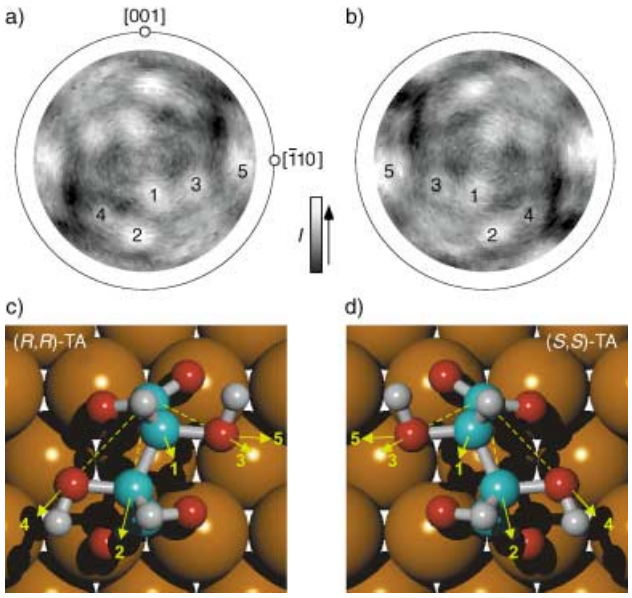

Figure 2. a), b): Experimental C1s XPD patterns from the (*R*,*R*)- and (*S*,*S*)-bitartrate species on Cu(110). The patterns are shown in stereographic projection and in a linear gray scale with white corresponding to maximum intensity. c), d): Molecular conformations deriving from a purely geometrical evaluation of the positions of the prominent forward-focusing maxima labeled 1–5 in (a) and (b).

In addition to the absolute configuration, detailed structural parameters can be determined by comparing the experimental XPD pattern to those obtained from calculations, systematically optimizing the structural parameters until best agreement is achieved. The relatively simple and efficient single-scattering cluster (SSC) formalism[13] has proven adequate in most cases, and in particular for molecular adsorbate systems.[17,18] Figure 3a defines the structural parameters α, β, and γ of the (*R*,*R*)-bitartrate molecule that we have varied in the SSC analysis. The initial bond lengths and bond angles were those typically found for the bitartrate ions in alkali-metal salts.[21] In a series of calculations we have varied the structural parameters in small steps and compared the resulting SSC diffraction patterns to the experimental XPD pattern from the (*R*,*R*)-enantiomer (Figure 2a). The agreement between simulated and experimental diffraction patterns was quantified using the reliability factor R_{MP}[22] A color-coded contour-plot of the resulting *R*-factor values as well as a top view of the best-fit molecular structure are shown in Figure 3c and b, respectively. The *R*-factor minimum of 0.078 is found at values of $21 \pm 4°$ for the carbon backbone torsion angle α and $24 \pm 4°$ for the deviation γ of the C2–C3 bond direction away from the [001] direction. The dependency of the *R*-factor from the carboxy group rotation angle β is too weak to allow a determination of β. This result is not unexpected since the oxygen atoms O1, O2, O5, and O6 binding to the Cu surface are located below the carbon photoemitters and thus do not contribute to the observed

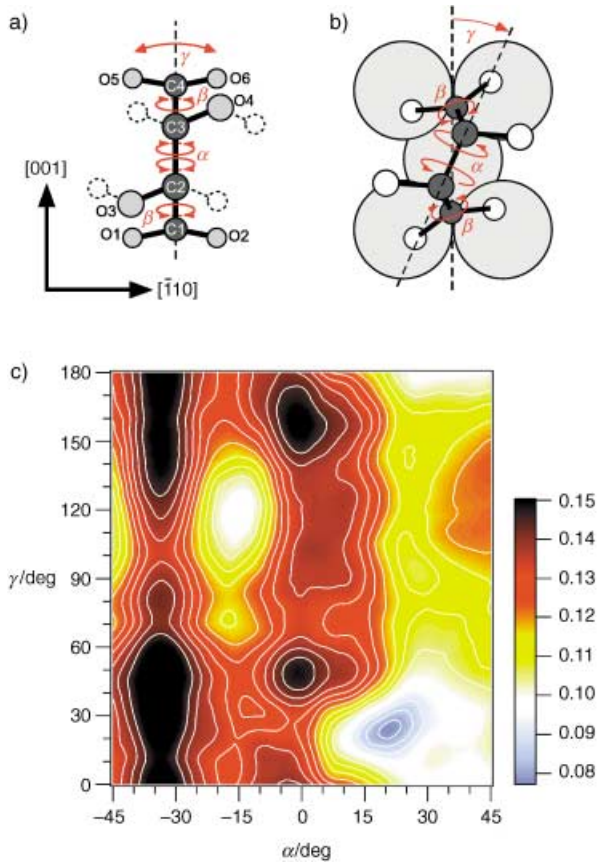

Figure 3. Determination of detailed structural parameters for the *R,R* enantiomer by means of SSC calculations. a) Schematic representation of the molecular geometry assumed as a starting point for the calculations. The two angular parameters α and β as well as the azimuthal orientation γ of the C2–C3 bond are varied. Hydrogen atoms are shown as broken circles since they do not contribute to the XPD anisotropy, and hence are not taken into account in the calculations. b) Top-view of the best-fit molecular conformation. c) Contour plot of the dependency of the *R* factor on the carbon-skeleton torsion angle α and the molecule azimuthal orientation γ. The *R* factor changes by 0.005 between contour lines. Best agreement between calculation and experiment (lowest *R*-factor) is found for $\alpha = 21 \pm 4°$ and $\gamma = 24 \pm 4°$.

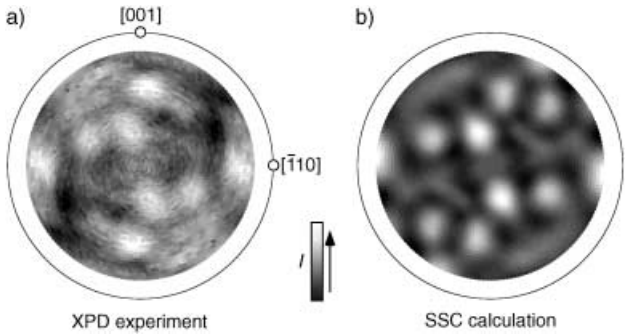

Figure 4. Comparison between experimental XPD pattern for the (*R,R*)-bitartrate (a) and best-fit calculation for the optimized molecular conformation shown in Figure 3b (b). The simulation accurately reproduces the experimental XPD pattern.

forward-focusing pattern.[23] For the geometry shown in Figure 3b all the carboxy group oxygen atoms are located an equal distance above the Cu surface, as previously concluded from IR spectroscopy studies,[14] which leads to a calculated β angle of 47.5° for the structure shown in Figure 3b.

This best-fit structure (Figure 3b) is identical to the structural model derived from the purely geometrical arguments (Figure 2c), thus yielding a consistent picture of the molecular conformation. Finally, the experimental (*R,R*)-tartaric acid C1s XPD pattern and the pattern obtained for the best-fit calculation are in excellent agreement (Figure 4). The calculation does not only reproduce the prominent forward-focusing maxima but also most of the fainter features of the intensity distribution. The remaining minor differences, in particular with respect to relative intensities, must be assigned to the known limitations of the SSC model.[24]

The conformation of the (*R,R*)-bitartrate enantiomer on Cu(110) as predicted from density functional theory (DFT) calculations is qualitatively similar to the one determined here, but with significantly smaller angular distortions.[25] The bitartrate model based on the above-mentioned IR investigation had all four carbon atoms positioned in a plane perpendicular to the surface.[14] A highly strained bitartrate, however, was proposed for the adsorbate complex on Ni(110).[26] On the other hand, enantiomorphous domains have been observed for the achiral bisuccinate species (OOC-CH_2-CH_2-COO) on Cu(110).[27] It must therefore be concluded that it becomes chiral upon adsorption, which can only be explained by an angular distortion of the molecular frame, as found here for bitartrate. Such conformational changes upon adsorption are driven by the energy balance between bonding to preferred substrate sites, intermolecular interactions, and the stability of the bonds in the adsorbate. Investigations on the change of molecular structure upon adsorption, as presented herein, therefore have the potential to give detailed insight into the mechanisms of molecular chemisorption and provide a stringent test for results obtained from DFT calculations. The only drawbacks of the XPD method are the need for a single crystalline substrate to align the majority of the molecules, and an ultrahigh vacuum environment to provide the mean free path for the photoelectrons.

In conclusion, we have demonstrated that angle-scanned XPD allows the handedness of adsorbed chiral molecules to be determined, and the enantiomers to be distinguished and identified in a straightforward way. The C1s XPD patterns from tartaric acid adsorbed on Cu(110) exhibit pronounced forward-focusing maxima owing to intramolecular scattering that directly yield the molecular conformation without the need for complex calculations. Using SSC calculations, the molecular distortions upon adsorption have been determined to a high degree of accuracy. With further increasing brilliance and stability of new synchrotron radiation sources it will become possible to achieve additional chemical sensitivity in XPD by selecting a specific chemically shifted core-level emission line. This opens the opportunity to selectively investigate the local geometrical environment of an element in different chemical surroundings within a molecule.

Experimental Section

(2*R*,3*R*)- and (2*S*,3*S*)-tartaric acid (Aldrich 99%) were evaporated from a Knudsen cell at 120°C in ultrahigh vacuum (UHV) onto a Cu(110) crystal held at 405 K. The formation of the ordered bitartrate structure was confirmed by low-energy electron diffraction (LEED) and photoelectron spectroscopy (XPS). The XPD experiments were performed at the Surface and Interface Microscopy Beamline of the Swiss Light Source using linearly polarized synchrotron X-ray radiation of 920 eV. The C 1s ($E_{kin} = 633$ eV) XPD patterns were collected with the sample held at room temperature.

Received: November 12, 2003 [Z53311]

Keywords: absolute configuration · chirality · molecular adsorption · photoelectron diffraction · surface chemistry

[1] a) L. Pasteur, *Ann. Chim. Phys.* **1848**, *24*, 442; b) J. H. van't Hoff, *Arch. Neerl. Sci. Exactes Nat.* **1874**, *9*, 445; c) J. A. le Bel, *Bull. Soc. Chim. Fr.* **1874**, *2*, 337.
[2] a) E. Fischer, *Ber. Dtsch. Chem. Ges.* **1891**, *24*, 2683; b) M. A. Rosanoff, *J. Am. Chem. Soc.* **1906**, *28*, 114.
[3] P. M. Bijvoet, A. F. Peerdman, A. J. van Bommel, *Nature* **1951**, *168*, 271.
[4] a) M. Carnell, S. D. Peyerimhoff, A. Breest, K. H. Gödderz, P. Ochmann, J. Hormes, *Chem. Phys. Lett.* **1991**, *180*, 477; b) F. J. Devlin, P. J. Stevens, J. R. Cheeseman, M. J. Frisch, *J. Am. Chem. Soc.* **1996**, *118*, 6327; c) J. Costante, L. Hecht, P. L. Polavarapu, A. Collet, L. D. Barron, *Angew. Chem.* **1997**, *109*, 917–919; *Angew. Chem. Int. Ed. Engl.* **1997**, *36*, 885.
[5] a) J.-L. Wang, M. Lahav, L. Leiserowitz, *Angew. Chem.* **1991**, *103*, 698–699; *Angew. Chem. Int. Ed. Engl.* **1991**, *30*, 696; b) L. Addadi, Z. Berkovics-Yellin, I. Weissbuch, M. Lahav, L. Leiserowitz, *Top. Stereochem.* **1986**, *16*, 1.
[6] D. M. Walba, H. A. Razavi, N. A. Clark, D. S. Parmar, *J. Am. Chem. Soc.* **1988**, *110*, 8686.
[7] a) L. Addadi, S. Weiner, *Nature* **2001**, *411*, 753; b) N. Bouropoulos, L. Addadi, S. Weiner, *Chem. Eur. J.* **2001**, *7*, 1881.
[8] a) *Chiral Reactions in Heterogeneous Catalysis* (Eds.: G. Jannes, V. Dubois), Plenum, New York, **1995**; b) H. U. Blaser, *Tetrahedron: Asymmetry* **1991**, *2*, 843; c) A. Baiker, H. U. Blaser in *Handbook of Heterogeneous Catalysis*, *Vol. 5* (Eds.: G. Ertl, H. Knözinger, J. Weitkamp), VCH, Weinheim, **1997**, p. 2422.
[9] a) Y. Izumi, *Adv. Catal.* **1983**, *32*, 215; b) G. Webb, P. B. Wells, *Catal. Today* **1992**, *12*, 319.
[10] R. Raval, *Nature* **2003**, *425*, 463.
[11] a) G. P. Lopinski, D. J. Moffatt, D. D. M. Wayner, R. A. Wolkow, *Nature* **1998**, *392*, 909; b) H. Fang, L. C. Giancarlo, G. W. Flynn, *J. Phys. Chem. B* **1998**, *102*, 7311.
[12] W. Hofer, *Prog. Surf. Sci.* **2003**, *71*, 147–183.
[13] C. S. Fadley in *Synchrotron Radiation Research: Advances in Surface Science*, *Vol. 1* (Ed.: R. Z. Bachrach), Plenum, New York, **1990**, pp. 421.
[14] M. Ortega Lorenzo, S. Haq, T. Bertrams, P. Murray, R. Raval, C. J. Baddeley, *J. Phys. Chem. B* **1999**, *103*, 10661.
[15] a) Contradicting terminologies for the deprotonated forms of tartraic acid are found in the literature. We use "bitartrate" for the form in which both carboxylic acid groups are deprotonated, as opposed to the "monotartrate" form in which only one acid group has deprotonated; b) M. Ortega Lorenzo, C. J. Baddeley, C. Muryn, R. Raval, *Nature* **2000**, *404*, 376.
[16] For reviews, see: a) J. Osterwalder, P. Aebi, R. Fasel, D. Naumovic, P. Schwaller, T. Kreutz, L. Schlapbach, T. Abukawa, S. Kono, *Surf. Sci.* **1995**, *331–333*, 1002; b) C. S. Fadley, *Prog. Surf. Sci.* **1997**, *54*, 341; c) C. Westphal, *Surf. Sci. Rep.* **2003**, *50*, 1.
[17] R. Fasel, A. Cossy, K.-H. Ernst, F. Baumberger, T. Greber, J. Osterwalder, *J. Chem. Phys.* **2001**, *115*, 1020.
[18] a) R. Fasel, P. Aebi, R. G. Agostino, D. Naumovic, J. Osterwalder, A. Santaniello, L. Schlapbach, *Phys. Rev. Lett.* **1996**, *76*, 4733; b) R. Fasel, unpublished results.
[19] J. Wider, M. Muntwiler, C. Quitmann, T. Greber, unpublished results.
[20] Because of their small photoelectron scattering cross section, the positions of the hydrogen-atoms can not be determined from XPD data. For the sake of clarity, however, hydrogen atoms have been added to the molecular skeleton in Figure 2c and d.
[21] a) V. S. Yadava, V. M. Padmanabhan, *Acta Crystallogr. Sect. B* **1973**, *29*, 493; b) G. K. Ambady, G. Kartha, *Acta Crystallogr. Sect. B* **1968**, *24*, 1540; c) H. Hinazumi, T. Mitsui, *Acta Crystallogr. Sect. B* **1972**, *28*, 3299.
[22] R. Fasel, P. Aebi, J. Osterwalder, L. Schlapbach, R. G. Agostino, G. Chiarello, *Phys. Rev. B* **1994**, *50*, 14516.
[23] A multiple-scattering analysis of low-energy C 1s XPD patterns would also allow the determination of the position of these oxygen atoms and hence β. This, however, is beyond the scope of the present work.
[24] R. D. Muino, D, Rolles, F. J. Garcia de Abajo, C. S. Fadley, M. A. Van Hove, *Surf. Rev. Lett.* **2002**, *9*, 1213.
[25] L. A. M. M. Barbosa, P. Sautet, *J. Am. Chem. Soc.* **2001**, *123*, 6639.
[26] V. Humblot, S. Haq, C. Muryn, W. A. Hofer, R. Raval, *J. Am. Chem. Soc.* **2002**, *124*, 503.
[27] S. M. Barlow, R. Raval, *Surf. Sci. Rep.* **2003**, *50*, 201.

